Communicated by Laurence Abbott

Reduction of Conductance-Based Models with Slow Synapses to Neural Nets

Bard Ermentrout
Dept. of Mathematics, University of Pittsburgh, Pittsburgh, PA 15260 USA

The method of averaging and a detailed bifurcation calculation are used to reduce a system of synaptically coupled neurons to a Hopfield type continuous time neural network. Due to some special properties of the bifurcation, explicit averaging is not required and the reduction becomes a simple algebraic problem. The resultant calculations show one how to derive a new type of "squashing function" whose properties are directly related to the detailed ionic mechanisms of the membrane. Frequency encoding as opposed to amplitude encoding emerges in a natural fashion from the theory. The full system and the reduced system are numerically compared.

1 Introduction

The appearance of large scale modeling tools for "biophysically realistic" models in neurobiology has led to increasingly complicated systems of nonlinear equations that defy any type of mathematical or heuristic analysis (Wilson and Bower 1989; Traub and Miles 1991). Supporters of this approach argue that all of the added complexity is necessary in order to produce results that can be matched to experimental data. In contrast are the very simple models that are based on firing rate (Hopfield and Tank 1986; Wilson and Cowan 1972), which are easily analyzed and computationally simple. These models inevitably invoke a sigmoid nonlinear transfer function for the current to firing rate relationship. The motivation for this is generally heuristic. In a recent paper, Rinzel and Frankel (1992) show that for some types of membrane models, one can explicitly derive neural network-like equations from the biophysics by averaging and assuming slow synapses. Our approach is similar with two important exceptions that we outline in detail below.

Consider the following system of coupled neurons:

$$C\frac{dV_j}{dt} + I_j^{\text{ion}}(V_j, \mathbf{w}_j) = \sum_k \lambda_{jk} s_k(t)(V_k^{\text{rev}} - V_j) + I_j^{\text{appl}} \tag{1.1}$$

$$\frac{d\mathbf{w}_j}{dt} = q(V_j, \mathbf{w}_j) \tag{1.2}$$

$$\frac{ds_j}{dt} = \epsilon[\hat{s}_j(V_j) - s_j] \tag{1.3}$$

The jth cell of the network is represented by its potential, V_j and all of the auxiliary channel variables that make up the dynamics for the membrane, $\mathbf{w}_j$. (For the Hodgkin–Huxley equations, these would be m, n, h.) The term I_j^{appl} is any tonic applied current. Finally, the synapses are modeled by simple first-order dynamics and act to hyperpolarize, shunt, or depolarize the postsynaptic cell. Associated with each neuron is a synaptic channel whose dynamics is governed by the variable s_j, which depends in a (generally nonlinear) manner on the somatic potential. Thus, one can think of s_j as being the fraction of open channels due to the presynaptic potential. The functions $\hat{s}_j$ have maxima of 1 and minima of 0. The effective maximal conductances of the synapses between the cells are in the nonnegative numbers λ_{jk} and the reversal potentials of each of the synapses are V_j^{rev}. Our goal is to derive equations that involve only the s_j variables and thus reduce the complexity of the model yet retain the qualitative (and perhaps quantitative) features of the original. (Note that we are explicitly assuming that the synapses from a given neuron, k, share the same synaptic dependencies, s_k. If this is unreasonable for a particular model, then one must include a different variable for each of the different synaptic dependencies of a given neuron. Nevertheless, the techniques of this article can still be used.)

The main idea is to exploit the smallness of ϵ and thus invoke the averaging theorem on the slow synaptic equations. Each of the slow synapses $s_1, \ldots, s_n$ is held constant and the membrane dynamics equations are solved for the potentials, $V_j(t; s_1, \ldots, s_n)$. The potentials, of course, naturally depend on the values of the synapses. We will assume that the potentials are either constant or periodic with period, $T(s_1, \ldots, s_n)$. (If they are constant, one can take $T = 1$ for example.) Once the potentials are found, one then averages the slow synaptic equations over one period of the membrane dynamics obtaining

$$\frac{ds_j}{dt} = \epsilon[S_j(s_1, \ldots, s_n) - s_j] \tag{1.4}$$

where

$$S_j(s_1, \ldots, s_n) = \frac{1}{T_j(s_1, \ldots, s_n)} \int_0^{T_j(s_1, \ldots, s_n)} \hat{s}_j[V_j(t; s_1, \ldots, s_n)]\, dt \tag{1.5}$$

Our goal is to explicitly derive expressions for these dependencies and to then compare the simplified or reduced system with the full model that includes all of the fast membrane dynamics.

Many synapses in the nervous system are not slow and others that are said to be slow are slow only in the sense that they have long lasting effects (see, e.g., Kandel *et al.* 1991, Chapter 11). Thus, one must view

this work as an approximation of what really happens and as a means of converting full spiking models to "firing rate" models while maintaining quantitative features of the latter. While we have explicitly assumed that the synapses are slow in order to derive the relevant equations, one does not need to be so specific as to the separation of time scales between spiking and synaptic activity. The main assumption is that the detailed phase and timing of individual spikes are not important, that is, one is free to average over many spiking events. If events are occurring far out on the dendritic tree, then the low-pass filtering properties of long dendrites act in a manner similar to "slow synapses." Thus, one should regard the assumption of slowness as sufficient but not necessary for the present reduction.

Rinzel and Frankel (1992) apply the same averaging methods to derive equations for a pair of mutually coupled neurons that was motivated by an experimental preparation. In their paper, they require only cross connections with no self-self interactions. Thus, they arrive at equations where V_j depends only on s_k where $j = 1, 2$. $k = 2$ for $j = 1$, and $k = 1$ for $j = 2$.

$$\frac{ds_j}{d\tau} = \hat{s}_j(s_k) - s_j \tag{1.6}$$

The key to their analysis is that they are able to numerically determine the potential as a function of the strength of the synapses. They use a class of membrane models that are called "class II" (see Rinzel and Ermentrout, 1989) where the transition from rest to repetitive firing occurs at a *subcritical* Hopf bifurcations and is typical of the Hodgkin–Huxley model (Hodgkin and Huxley 1952). This latter assumption implies that the average potential exhibits hysteresis as a function of the synaptic drive. That is the functions $\hat{s}_j(s_k)$ are multivalued for some interval of values of s_k. Because of this hysteresis, they are able to combine an excitatory cell and an inhibitory cell in a network as shown in Figure 1 and obtain oscillations. It is well known that for smooth single valued functions $\hat{s}_j$ oscillations are impossible without self-excitatory interactions (see, e.g., Rinzel and Ermentrout 1989). If, however, one generalizes their approach to include more than one type of synapse per cell or the addition of applied currents, then it is necessary to compute the voltages for each set of possible synaptic values. This is a formidable numerical task. The other feature of the Rinzel–Frankel analysis is that the nonlinearity $\hat{s}_j$ does not look like a typical Hopfield or Wilson–Cowan squashing function due to the hysteresis phenomenon. This hysteresis can be avoided if the bifurcation to periodic solutions is *supercritical* but then there are very delicate problems as the synapses slowly pass through the bifurcation point (Baer *et al.* 1989). (In fact, in this slow passage problem occurs in the subcritical case as well; the authors avoid its consequences by adding a small amount of noise to the simulations.) Finally, in class II

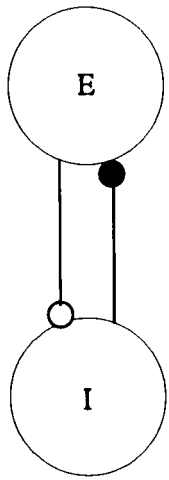

Figure 1: Two-cell network with reciprocal connections. No self-connections are allowed.

membranes, the dependence of the frequency on the level of depolarization is discontinuous and essentially piecewise quadratic. The amplitude of the potential varies in a piecewise linear fashion. (See Figure 5.2 in Rinzel and Ermentrout 1989.) Thus, the values of s_j in the Rinzel–Frankel model are not explicitly tied to the *frequency* of the impulses as they are to the averaged magnitude of the potential.

In this paper, we consider use of "class I" models of membranes instead of "class II" membranes as the basis for the averaging. We show that this will lead to a simpler form for the synaptic equations with the added benefits of (1) obviating the complicated mathematical difficulties while passing through the transition from rest to repetitive firing; (2) suggesting a natural form for the squashing function that is monotone increasing and that is very similar to the firing rate curves of some cortical neurons; and (3) making very explicit the frequency encoding properties of the active membrane. Note that this reduction requires that the membrane actually exhibit class I dynamics and in those systems in which class II dynamics occurs, the Rinzel–Frankel reduction is appropriate.

In Section 2, we review the membrane dynamics and show how the necessary averages can be approximated by a simple algebraic expression. We then apply this to a two-layer model with self-excitation and self-inhibition as well as crossed connections. Comparisons between the full and the reduced models are given in the last section.

2 Class I Dynamics and Firing Rates

Rinzel and Ermentrout (1989) contrast the difference between class II and class I membranes. The former include the well-known Hodgkin–Huxley model while the latter include the model of Connor as well as models of cortical cells with A currents (L. Abbott, personal communication). Class II axons have a transition from rest to repetitive firing that arises from a Hopf bifurcation. As a consequence, the frequency goes from 0 spikes per second to some finite nonzero rate and the average of the potential (in the case of Rinzel and Frankel) has a discontinuous jump. As we discussed previously, there is hysteresis so that the average value of the potential is as shown in Figure 2a.

In contrast to the dynamics of class II membranes, class I membranes have a continuous transition from nonspiking to spiking both in the average potential and in the firing rate of the membrane (see Fig. 2b). A general analysis of this type of bifurcation is given in Ermentrout and Kopell (1986) with particular attention paid to slowly perturbed neural

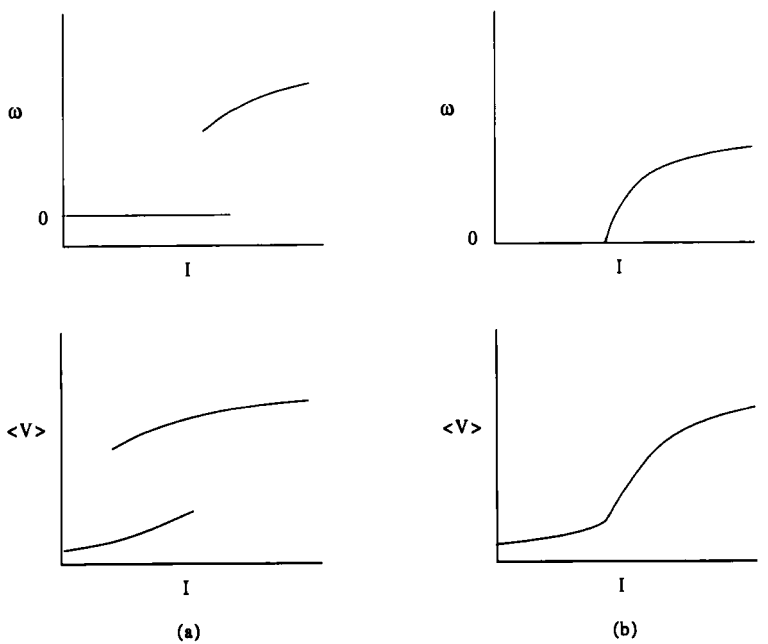

Figure 2: Average potential and frequency of firing as a function of current for (a) class II membranes; (b) class I membranes.

models (precisely what we have here). In particular, we show that the frequency of the periodic orbit is

$$\omega = C(p^*)\sqrt{[p - p^*]_+} + O(|p - p^*|) \tag{2.1}$$

where p is any parameter such that as p increases from below p^*, the membrane switches into oscillations. (Here, $[z]_+ = z$ if $z > 0$ and vanishes for $z < 0$.) There are several important advantages of this type of relation in so far as coding of information by firing rate is concerned. First, the network is extremely sensitive near threshold and thus a very large range of firing rates is possible. This behavior is typical in continuous but nondifferentiable firing rate models. Second, slowly varying the parameter p yields the intuitively expected behavior of slowly varying the firing rate even as one crosses the critical regime (cf. Ermentrout and Kopell 1986, Lemma 1). In contrast, with a class II membrane, there is bistability and thus an instant jump from no firing to nearly maximal firing and a ramping effect whereby the system may remain very close to rest even though the slowly moving parameter is well past criticality (see Baer *et al.* 1989).

One can object that the computational problem of finding the average of the potential as a function of many possible parameters still exists. However, as we will see, it turns out that the parametric computation of the periodic solutions for the membrane can actually be reduced to an algebraic computation of equilibria near criticality. Thus, the computation of hundreds of periodic orbits is no longer necessary. Because of the special form of the membrane potential, the algebraic calculation is one of finding fixed points to a *scalar* equation!

Recall from 1.3 that $\hat{s}$ is the function that determines the fraction of open channels as a function of the presynaptic potential. This is generally a function of the potential, for example, $\hat{s}(V) = [\tanh[\sigma(V - V_{\text{th}})]]_+$. Here σ is the sharpness of the nonlinearity. Consider the averaged synaptic function:

$$S(p) = \frac{1}{T(p)} \int_0^{T(p)} \hat{s}[V(t;p)]\, dt \tag{2.2}$$

where p is a critical parameter on which the potential depends. Suppose that $\hat{s}$ is 0 if the membrane is at rest (and thus below threshold) and 1 if the voltage is above threshold (e.g., σ is very large). Let $\xi(p)$ denote the amount of time during one cycle that the potential is above threshold. Then, 2.2 is simplified to

$$S(p) = \frac{\omega(p)\xi(p)}{2\pi} \tag{2.3}$$

where we have used the fact that $T = 2\pi/\omega$. A fortuitous property of class I membranes is that the time for which the spike is above threshold is largely independent of the period of the spike so that $\xi(p)$ is essentially constant. (This is certainly true near threshold and we have found it to

be empirically valid in a wide parameter range.) Thus, combining this with 2.1, we obtain the very simple squashing function:

$$S(p) = C(p^*)\sqrt{([p - p^*]_+)} \tag{2.4}$$

where $C(p)$ and of course p^* depend on the other parameters in the model. In deriving 2.4 we have made two simplifications: (1) the actual frequency is of the form 2.1 only near criticality and (2) the synaptic function $\hat{s}$ may be more graded than a simple on/off. The first simplification seems to be pretty reasonable; prior calculations (see Rinzel and Ermentrout 1989) indicate the square-root relationship holds over a wide range of the parameter. The second simplification is not particularly important as the main effect is to slightly change the constant $C(p^*)$.

The squashing function is completely determined if we can compute p^* and $C(p^*)$ as a function of all of the remaining parameters in the membrane. As we remarked in the above paragraph, the actual constant $C(p^*)$ is not that important, so that the crucial calculation is to find the critical value p^* as a function of the remaining parameters. Since only the injected currents and the other synapses will be variable, we can limit the number of parameters to vary. In the next section, we compute p^* and thus obtain a closed form equation for the synaptic activities.

3 Computation of the Squashing Function for a Simple Model

In this section, we detail the calculations of p^* and $C(p^*)$ for the dimensionless Morris–Lecar membrane model (see Rinzel and Ermentrout 1989; Morris and Lecar 1981) with excitatory and inhibitory synapses and injected current. The explicit dimensionless equations are

$$\frac{dV}{dt} = I + g_e(V_e - V) + g_i(V_i - V) + I_{ion}(V, w) \tag{3.1}$$

$$\frac{dw}{dt} = \frac{w_\infty(V) - w}{\tau_w(V)} \tag{3.2}$$

where

$$\begin{aligned} I_{ion}(V, w) &= m_\infty(V)(1 - V) + 0.5(-0.5 - V) + 2w(-0.7 - V) \\ m_\infty(V) &= 0.5(1 + \tanh[(V + 0.01)/0.15]) \\ w_\infty(V) &= 0.5(1 + \tanh[(V - 0.05)/0.1]) \\ \tau_w(V) &= 1/(3\cosh[(V - 0.05)/0.2)]) \end{aligned}$$

and $V_e = 1$, $V_i = -0.7$.

The transition from rest to oscillation occurs in class I membranes via a saddle-node bifurcation of an equilibrium. Thus, if the differential equation is

$$\frac{dx}{dt} = f(x, p)$$

we want to solve $f(x, p^*) = 0$ where $x = x(p)$ is a vector of rest states depending on p such that the determinant of the Jacobi matrix of f with respect to x evaluated at $x(p^*)$ is zero (see Guckenheimer and Holmes 1983). For membrane models, this is very simple. Let V denote the membrane potential and w denote the gating variable(s). Each of the gating variables is set to its steady state value, $w = w_\infty(V)$ and thus the equilibrium for the voltage satisfies

$$0 = I^{\text{ionic}}[V, w_\infty(V)] + g_e(V_e - V) + g_i(V_i - V) + I \tag{3.3}$$

where g_e and g_i are the total excitatory and inhibitory conductances, V_j are the reversal potentials, and I is the total applied current. For each (g_e, g_i, I) we find a rest state, $\bar{V}$. Next, we want this to be a saddle-node point, so we want the derivative of this function to vanish:

$$0 = \frac{dI^{\text{ionic}}[V, w_\infty(V)]}{dV} - g_e - g_i \tag{3.4}$$

Suppose we want to view g_e as the parameter that moves us from rest to repetitive firing. Then, we can solve 3.3 for $g_e(V, I, g_i)$, substitute it into 3.4, and use a root finder to get the critical value of V^* and thus g_e^*. This is a simple algebraic calculation and results in $g_e^*(g_i, I)$, a two-parameter surface of critical values of the excitatory conductance. A local bifurcation analysis at this point enables us to compute $C(p^*)$ as well. (The local bifurcation calculation is tedious but routine (see Guckenheimer and Holmes 1983) and involves no more than a few Taylor series terms of the nonlinearities and some trivial linear algebra. In particular, no numerical calculations of periodic orbits are required.) The end result of this calculation is shown in Figure 3a,b. The figure for the critical value of the excitatory conductance suggests that the relationship between it and the parameters g_i and I is almost linear. We have used a least squares fit of this and find that

$$g_e^*(g_i, I) \approx a + bI + cg_i + dIg_i \tag{3.5}$$

where $a = 0.02316$, $b = -0.7689$, $c = 0.3468$, $d = -0.1694$. Note that the dependence is not strictly linear; there is a small interaction term of the inhibitory conductance with the current.

Using this we can obtain the slow equations for a Wilson–Cowan type two-cell network of excitatory and inhibitory cells with self-excitatory connections (in contrast to Fig. 1). The conductances are related to the synapses by the relations, $g_{\alpha\beta} = \lambda_{\alpha\beta} s_\alpha$ where α, β are either e or i. Thus, we arrive at the coupled network:

$$\tau_e \frac{ds_e}{dt} + s_e = C_e \sqrt{[\lambda_{ee} s_e - g_e^*(\lambda_{ie} s_i, I_e)]_+} \tag{3.6}$$

$$\tau_i \frac{ds_i}{dt} + s_i = C_i \sqrt{[\lambda_{ei} s_e - g_e^*(\lambda_{ii} s_i, I_i)]_+} \tag{3.7}$$

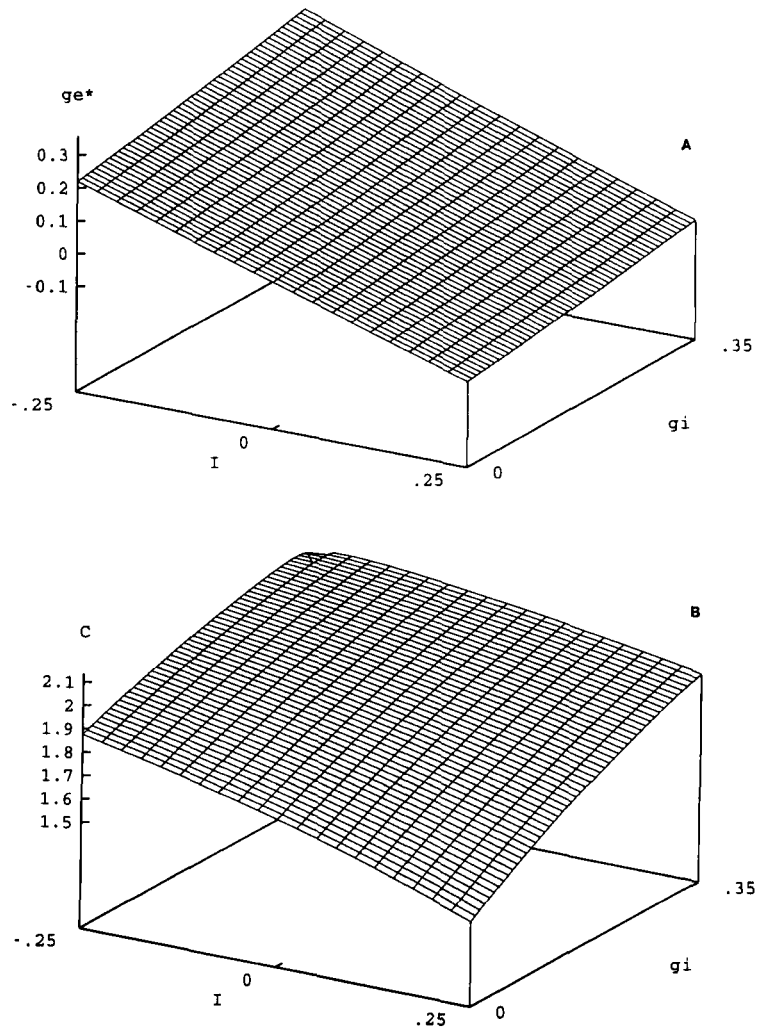

Figure 3: Critical surface (a) and bifurcation coefficient (b) for dimensionless Morris–Lecar model (3.1).

Note that C_e and C_i also depend on g_e^* so that the dependence is not strictly a square-root. However, as illustrated in Figure 3b, the bifurcation coefficient is close to constant, so that throughout the rest of this paper, we have chosen it as such. Note that the equations are not strictly additive as would be the case in a "pure" Hopfield network. This is be-

cause the inhibitory interactions are not just the negative of the excitatory interactions. Both are multiplied by their respective reversal potentials. Also, note that one does not have to compute the critical point with respect to g_e and could just as easily compute it with respect to some other parameter such as g_i. The function g_e^* is the critical value of excitatory conductance as a function of all of the other parameters and thus there is no "symmetry" in the notation for the two equations (3.6, 3.7).

Since the computation of g_e^* is purely local (that is, we need only compute rest states and their stability) for any given model, we can find g_e^* as a function of g_i and I. Once this is done, a curve fitting algorithm can be used to approximate the surface. Finally, the results can be substituted into 3.6–3.7 to arrive at a neural network model that is directly derived from the biophysical parameters. If one wishes to investigate a large network of such neurons, then the calculation remains simple as long as the only *types* of synapses are excitatory and inhibitory. As different synaptic types are added, one must compute g_e^* as a function of these additional parameters. Because the global rhythmic behavior of class I membranes is so stereotypical (at least, near threshold, and for many models, well beyond threshold), it is unnecessary to compute the dynamic periodic solutions numerically and so the computational complexity is reduced considerably.

There is no obvious manner in which the present computation could be extended to neurons that intrinsically burst or that have slow modulatory processes such as spike adaptation. However, such slow modulatory processes could be incorporated into the dynamic equations along with the firing rate equations. The reduction would then no longer lead to a single equation for each neuron, but rather several corresponding to each of the modulatory dynamic variables.

4 Some Numerical Comparisons

In this section, we compare the simplified dynamics with the membrane models. In particular, the simple models predict the onset of oscillations in the firing rate of the full system (bursting) as well as transient excitation and bistability. As a final calculation, we illustrate spatial patterning in a two-layer multineuron network and compare it to a reduced model of the same type. For the present calculations, we have set the Morris–Lecar parameters as in Figure 3 and varied only the synaptic time constants τ_e, τ_i, currents, I_e, I_i, and weights, λ_{jk}.

In Figure 4, a typical nullcline configuration for 3.6 and 3.7 is shown when there is a unique steady state. If τ_i is not too small, then it is unstable and as can be seen in the figure, there is a stable periodic solution. Using the same values of the network parameters, we integrate 1.1 with $\epsilon = 0.01$. Figure 5 shows the phase-portrait of the averaged and the full models. There is good agreement in the shape of the oscillation.

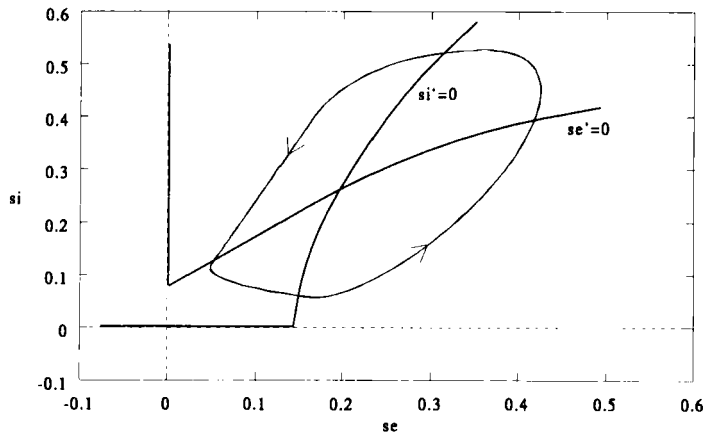

Figure 4: Nullclines and trajectory for 3.6–3.7. Nullclines are shown in dark lines, trajectory in light lines. Parameters are $\tau_e = \tau_i = 1$, $I_e = 0.05$, $I_i = -0.1$, and $\lambda_{ee} = 0.5$, $\lambda_{ei} = 0.6$, $\lambda_{ie} = 1$, $\lambda_{ii} = 0$.

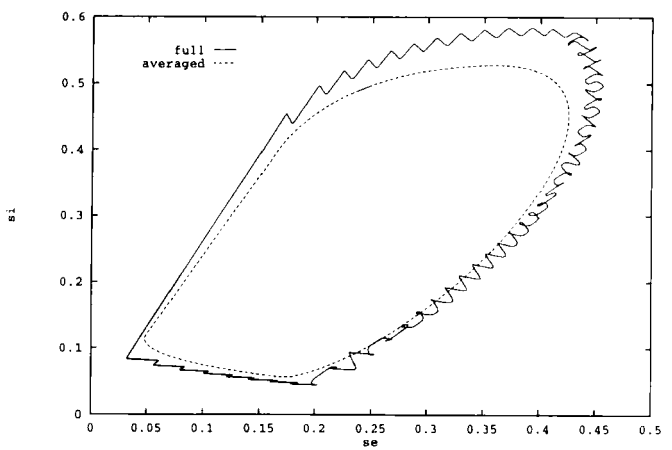

Figure 5: Phase-plane comparing full and averaged models for parameters of Figures 3 and 4.

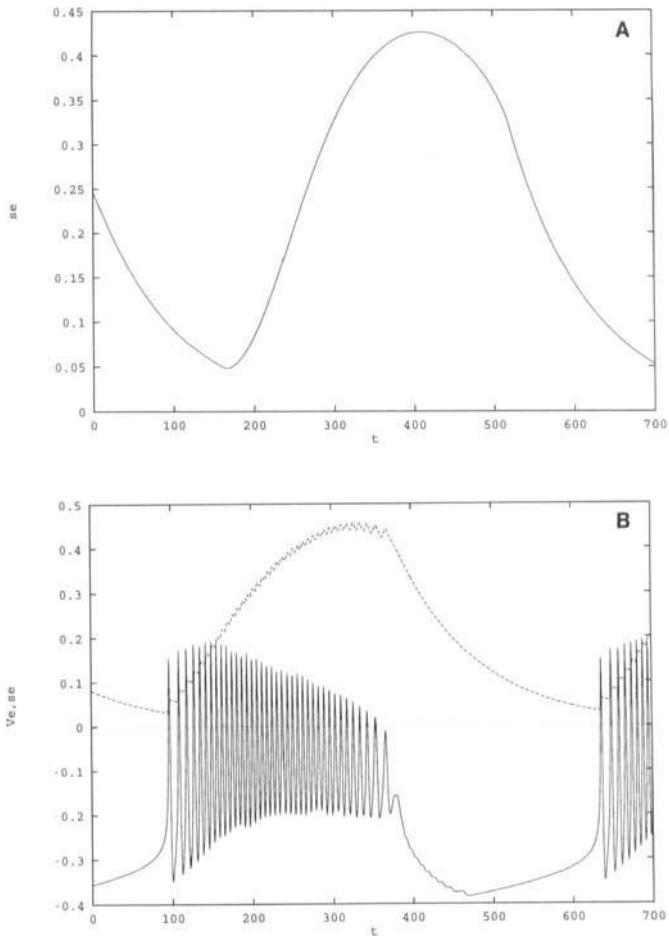

Figure 6: Time course of (a) full model showing excitatory potential and synaptic activity; (b) reduced model showing excitatory synaptic activity.

Figure 6b shows the time course of s_e for the averaged equations and Figure 6a shows that of V_e and s_e for the full model. The slow oscillation of the synaptic activities is reflected by the bursting activity of the potential. One point that is evident is that the period of the full oscillation is roughly the same as that of the averaged. Indeed, the period of the full model is about 5.405 and that of the averaged is 5.45 (in slow time units).

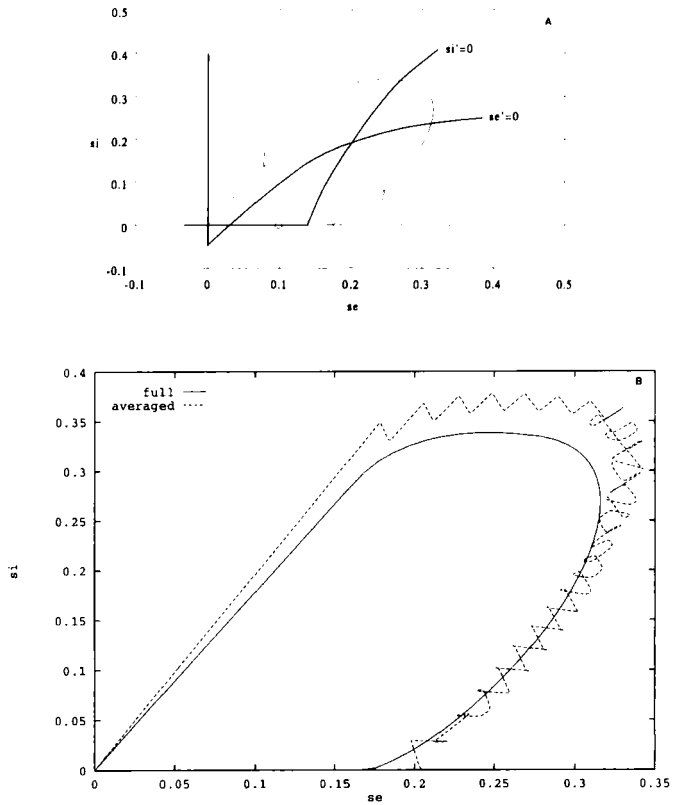

Figure 7: (a) Nullclines and trajectory for 3.6–3.7 in the excitable regime. Parameters as in Figure 4 except that $I_e = 0.0$. Circle indicates the initial condition. (b) Comparison of phase-plane of full and reduced models.

Thus, not only is there qualitative agreement, but quantitative agreement between the full and reduced models.

Figure 7a shows the nullclines and phase-plane for a set of parameters for which the reduced model is either excitable ($\tau_i \approx 1$) or bistable ($\tau_i \ll 1$). Figure 7b compares the phase-planes of the full and reduced models in the excitable regime. In the bistable regime, one finds that the potentials exist either silently or in an oscillatory mode corresponding to the upper steady state of the synaptic activities. The reduced model is a good predictor of transient activity as well as the sustained bursting shown in the previous example.

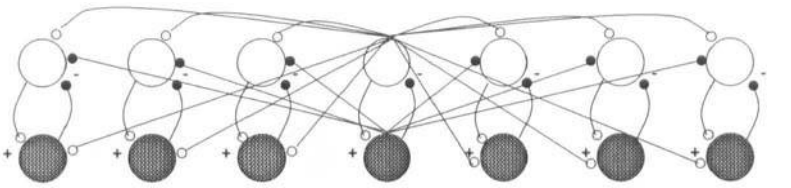

Figure 8: Schematic of a network of connected cells in a ring.

As a final simulation that truly illustrates the power of the method, we consider a two-layer network of 20 cells coupled in a ring of length 2π as shown in Figure 8. The network equations for the reduced model have the form:

$$\tau_e \frac{ds_e^j}{dt} + s_e^j = C_e \sqrt{\left[\lambda_{ee} \sum_k w_e(j-k) s_e^k - g_e^* \left(\lambda_{ie} \sum_k w_i(j-k) s_i, I_e\right)\right]_+} \tag{4.1}$$

$$\tau_i \frac{ds_i^j}{dt} + s_i^j = C_i \sqrt{\left[\lambda_{ei} \sum_k w_e(j-k) s_e^k - g_e^* \left(\lambda_{ii} \sum_k w_i(j-k) s_i^k, I_i\right)\right]_+} \tag{4.2}$$

Here w_e and w_i are periodized gaussian weights

$$w_\alpha(j) = B_\alpha \sum_{n=-\infty}^{\infty} \exp\left(-\frac{j+2\pi n^2}{\sigma_\alpha}\right)$$

where α is either e or i and the constants B_α are chosen so that $\sum_{n=-\infty}^{\infty} w_\alpha(n) = 1$. Setting $\sigma_e = 0.5$ and $\sigma_i = 2.0$ we obtain a network with lateral inhibitory properties. The parameters I_e and I_i are externally applied stimuli to the network. This network is integrated numerically starting with initial data with two peaks and a random perturbation. The steady state spatial profiles of the reduced and the averaged models are shown in Figure 9a. The spacing, width, and height of the peaks agree well between the two regimes. Figure 9b shows a space-time plot of the potentials of the excitatory cells in the fast time scale (thus showing the individual spikes of the active region). The strip is broken into spatially distinct regimes of oscillatory and silent cells.

These simulations show that there is very good qualitative and even quantitative agreement between the reduced system and the full model

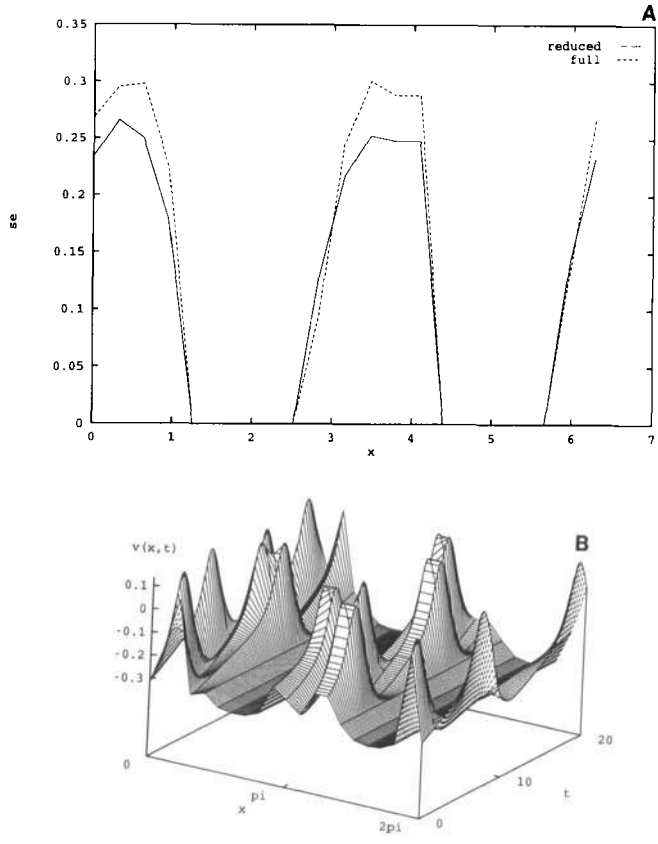

Figure 9: Simulation of the ring. Parameters are $\tau_e = \tau_i = 1$. $I_e = 0.1$, $I_i = 0$. and $\lambda_{ee} = 0.2$, $\lambda_{ei} = 0.6$, $\lambda_{ie} = 0.8$, $\lambda_{ii} = 0$. (a) Spatial profile of the reduced and full excitatory synaptic activity. (b) Potential of the excitatory cell as a function of space and time. (Note that this is in the fast time-scale so that individual spikes can be seen in the active regions.)

for simple two-cell networks as well as for spatially extended systems. There is a huge increase in computational speed for the simplified models and thus one can use them to find "interesting" parameter ranges before attempting to simulate the full model.

The main feature of this method is that it makes explicit the dependence of the frequency encoding of a neuron on its biophysical properties. By using membranes with so-called class I excitability, the actual computation of the reduced models is reduced to an algebraic problem in

combination with a curve fitting algorithm. We suggest that to the usual types of squashing functions seen in the neural network literature, one add the square-root model since it can be explicitly derived from the conductance properties of nerve membranes. We finally want to point out that this reduction justifies the use of so-called connectionist models under the assumptions that the synaptic interactions are *slow* compared to the ionic flows in the membrane. Furthermore, the time scales of the present reduced models are *not* those of the membrane time constant to which many of the Hopfield models refer. Nevertheless, many neuronal processes occur at time scales slower than the action potentials; thus our technique can be useful in understanding these phenomena.

Acknowledgments

Supported in part by NIMH-47150, NSF (DMS-9002028).

References

Baer, S. M., Erneux, T., and Rinzel, J. 1989. The slow passage through a Hopf bifurcation: Delay, memory effects, and resonance. *SIAM J. Appl. Math.* **49**, 55–71.

Connor, J. A., Walter, D., and McKown, R. 1977. Neural repetitive firing: Modifications of the Hodgkin-Huxley axon suggested by experimental results from crustacean axons. *Biophys. J.* **18**, 81–102.

Ermentrout, G. B., and Kopell, N. K. 1986. Parabolic bursting in an excitable system coupled with a slow oscillation. *SIAM J. Appl. Math.* **46**, 233–253.

Guckenheimer, J., and Holmes, P. 1983. *Nonlinear Oscillations, Dynamical Systems, and Bifurcations of Vector Fields.* Springer-Verlag, New York.

Hodgkin, A. L., and Huxley, A. F. 1952. A quantitative description of membrane current and its application to conduction and excitation in nerve. *J. Physiol. (London)* **117**, 500–544.

Hopfield, J. J., and Tank, D. W. 1986. Computing with neural circuits: A model. *Science* **233**, 625–633.

Kandel, E., Schwartz, J. H., and Jessel, T. M. 1991. *Principles of Neural Science.* Elsevier, New York.

Morris, C., and Lecar, H. 1981. Voltage oscillations in the barnacle giant muscle fiber. *Biophys. J.* **35**, 193–213.

Rinzel, J., and Ermentrout, G. B. 1989. Analysis of neural excitability and oscillations. In *Method of Neuronal Modeling*, C. Koch and I. Segev, eds., pp. 135–171. MIT Press, Cambridge, MA.

Rinzel, J., and Frankel, P. 1992. Activity patterns of a slow synapse network predicted by explicitly averaging spike dynamics. *Neural Comp.* **4**, 534–545.

Traub, R., and Miles, R. 1991. *Neuronal Networks of the Hippocampus.* Cambridge University Press, Cambridge, UK.

Wilson, M. A., and Bower, J. M. 1989. The simulation of large-scale neural networks. In *Method of Neuronal Modeling*, C. Koch and I. Segev, eds., pp. 295–341. MIT Press, Cambridge, MA.

Wilson, H. R., and Cowan, J. D. 1972. Excitatory and inhibitory interactions in localized populations of model neurons. *Biophys. J.* **12**, 1–24.

Received July 9, 1993; accepted November 4, 1993.

This article has been cited by:

1. Haim Sompolinsky. 2014. Computational neuroscience: beyond the local circuit. *Current Opinion in Neurobiology* **25**, xiii-xviii. [CrossRef]
2. Paul C. Bressloff, Jay M. Newby. 2014. Path integrals and large deviations in stochastic hybrid systems. *Physical Review E* **89**. . [CrossRef]
3. Takuma Tanaka. 2014. Solvable model of the collective motion of heterogeneous particles interacting on a sphere. *New Journal of Physics* **16**, 023016. [CrossRef]
4. Paul C. Bressloff, Jay M. Newby. 2013. Metastability in a Stochastic Neural Network Modeled as a Velocity Jump Markov Process. *SIAM Journal on Applied Dynamical Systems* **12**, 1394-1435. [CrossRef]
5. Nicolas BrunelDynamics of Neural Networks 489-512. [CrossRef]
6. Y. Qi, A. L. Watts, J. W. Kim, P. A. Robinson. 2013. Firing patterns in a conductance-based neuron model: bifurcation, phase diagram, and chaos. *Biological Cybernetics* **107**, 15-24. [CrossRef]
7. P.A. Robinson, J.W. Kim. 2012. Spike, rate, field, and hybrid methods for treating neuronal dynamics and interactions. *Journal of Neuroscience Methods* **205**, 283-294. [CrossRef]
8. Paul C Bressloff. 2012. Spatiotemporal dynamics of continuum neural fields. *Journal of Physics A: Mathematical and Theoretical* **45**, 033001. [CrossRef]
9. Kenneth D. Miller, Francesco Fumarola. 2012. Mathematical Equivalence of Two Common Forms of Firing Rate Models of Neural Networks. *Neural Computation* **24**:1, 25-31. [Abstract] [Full Text] [PDF] [PDF Plus]
10. Emre Neftci, Elisabetta Chicca, Giacomo Indiveri, Rodney Douglas. 2011. A Systematic Method for Configuring VLSI Networks of Spiking Neurons. *Neural Computation* **23**:10, 2457-2497. [Abstract] [Full Text] [PDF] [PDF Plus]
11. Dipanjan Roy, Anandamohan Ghosh, Viktor K. Jirsa. 2011. Phase description of spiking neuron networks with global electric and synaptic coupling. *Physical Review E* **83**. . [CrossRef]
12. Carlo R. Laing, Thomas Frewen, Ioannis G. Kevrekidis. 2010. Reduced models for binocular rivalry. *Journal of Computational Neuroscience* **28**, 459-476. [CrossRef]
13. Serafim Rodrigues, Anton V. Chizhov, Frank Marten, John R. Terry. 2010. Mappings between a macroscopic neural-mass model and a reduced conductance-based model. *Biological Cybernetics* **102**, 361-371. [CrossRef]
14. P. D'Souza, S.-C. Liu, R. H. R. Hahnloser. 2010. Perceptron learning rule derived from spike-frequency adaptation and spike-time-dependent plasticity. *Proceedings of the National Academy of Sciences* **107**, 4722-4727. [CrossRef]
15. Hideo Hasegawa. 2008. Synchrony and variability induced by spatially correlated additive and multiplicative noise in the coupled Langevin model. *Physical Review E* **78**. . [CrossRef]

16. Boris B. Vladimirski, Joël Tabak, Michael J. O'Donovan, John Rinzel. 2008. Episodic activity in a heterogeneous excitatory network, from spiking neurons to mean field. *Journal of Computational Neuroscience* **25**, 39-63. [CrossRef]
17. Christian K. Machens, Carlos D. Brody. 2008. Design of Continuous Attractor Networks with Monotonic Tuning Using a Symmetry Principle. *Neural Computation* **20**:2, 452-485. [Abstract] [PDF] [PDF Plus]
18. Hideo Hasegawa. 2007. Generalized rate-code model for neuron ensembles with finite populations. *Physical Review E* **75**. . [CrossRef]
19. Bard Ermentrout. 2006. Gap junctions destroy persistent states in excitatory networks. *Physical Review E* **74**. . [CrossRef]
20. Bard ErmentroutNeural Behavior: Mathematical Models . [CrossRef]
21. Tadashi Yamazaki, Shigeru Tanaka. 2005. Neural Modeling of an Internal Clock. *Neural Computation* **17**:5, 1032-1058. [Abstract] [PDF] [PDF Plus]
22. ERIC BROWN, JUAN GAO, PHILIP HOLMES, RAFAL BOGACZ, MARK GILZENRAT, JONATHAN D. COHEN. 2005. SIMPLE NEURAL NETWORKS THAT OPTIMIZE DECISIONS. *International Journal of Bifurcation and Chaos* **15**, 803-826. [CrossRef]
23. H. Sompolinsky, O.L. WhiteCourse 8 Theory of large recurrent networks: From spikes to behavior 267-340. [CrossRef]
24. A. Hutt. 2004. Effects of nonlocal feedback on traveling fronts in neural fields subject to transmission delay. *Physical Review E* **70**. . [CrossRef]
25. Carlo R. Laing, André Longtin. 2003. Dynamics of Deterministic and Stochastic Paired Excitatory—Inhibitory Delayed Feedback. *Neural Computation* **15**:12, 2779-2822. [Abstract] [PDF] [PDF Plus]
26. Barbara J. Breen, William C. Gerken, Robert J. Butera, Jr.. 2003. Hybrid Integrate-and-Fire Model of a Bursting Neuron. *Neural Computation* **15**:12, 2843-2862. [Abstract] [PDF] [PDF Plus]
27. Bard Ermentrout. 2003. Dynamical Consequences of Fast-Rising, Slow-Decaying Synapses in Neuronal Networks. *Neural Computation* **15**:11, 2483-2522. [Abstract] [PDF] [PDF Plus]
28. Walter J. Freeman. 2003. A Neurobiological Theory of Meaning in Perception Part I: Information and Meaning in Nonconvergent and Nonlocal Brain Dynamics. *International Journal of Bifurcation and Chaos* **13**, 2493-2511. [CrossRef]
29. R.H.R. Hahnloser. 2003. Emergence of neural integration in the head-direction system by visual supervision. *Neuroscience* **120**, 877-891. [CrossRef]
30. Oren Shriki, David Hansel, Haim Sompolinsky. 2003. Rate Models for Conductance-Based Cortical Neuronal Networks. *Neural Computation* **15**:8, 1809-1841. [Abstract] [PDF] [PDF Plus]
31. K. Kang, M. Shelley, H. Sompolinsky. 2003. Mexican hats and pinwheels in visual cortex. *Proceedings of the National Academy of Sciences* **100**, 2848-2853. [CrossRef]

32. Richard H. R. Hahnloser, H. Sebastian Seung, Jean-Jacques Slotine. 2003. Permitted and Forbidden Sets in Symmetric Threshold-Linear Networks. *Neural Computation* **15**:3, 621-638. [Abstract] [PDF] [PDF Plus]

33. D. Hansel, G. Mato. 2003. Asynchronous States and the Emergence of Synchrony in Large Networks of Interacting Excitatory and Inhibitory Neurons. *Neural Computation* **15**:1, 1-56. [Abstract] [PDF] [PDF Plus]

34. Eugene M. Izhikevich, Frank C. Hoppensteadt. 2003. Slowly Coupled Oscillators: Phase Dynamics and Synchronization. *SIAM Journal on Applied Mathematics* **63**, 1935-1953. [CrossRef]

35. Xiaohui Xie, Richard Hahnloser, H. Seung. 2002. Double-ring network model of the head-direction system. *Physical Review E* **66**. . [CrossRef]

36. C. van Vreeswijk, D. Hansel. 2001. Patterns of Synchrony in Neural Networks with Spike Adaptation. *Neural Computation* **13**:5, 959-992. [Abstract] [PDF] [PDF Plus]

37. Marius Usher, James L. McClelland. 2001. The time course of perceptual choice: The leaky, competing accumulator model. *Psychological Review* **108**, 550-592. [CrossRef]

38. D. Golomb, D. Hansel, G. MatoChapter 21 Mechanisms of synchrony of neural activity in large networks 887-968. [CrossRef]

39. David J. Pinto, G. Bard Ermentrout. 2001. Spatially Structured Activity in Synaptically Coupled Neuronal Networks: I. Traveling Fronts and Pulses. *SIAM Journal on Applied Mathematics* **62**, 206-225. [CrossRef]

40. Mónica Romeo, Christopher Jones. 2000. Stability of neuronal pulses composed of concatenated unstable kinks. *Physical Review E* **63**. . [CrossRef]

41. H SEUNG. 2000. Stability of the Memory of Eye Position in a Recurrent Network of Conductance-Based Model Neurons. *Neuron* **26**, 259-271. [CrossRef]

42. Paul C. Bressloff, S. Coombes. 2000. Dynamics of Strongly Coupled Spiking Neurons. *Neural Computation* **12**:1, 91-129. [Abstract] [PDF] [PDF Plus]

43. P. C. Bressloff, S. Coombes. 2000. A Dynamical Theory of Spike Train Transitions in Networks of Integrate-and-Fire Oscillators. *SIAM Journal on Applied Mathematics* **60**, 820-841. [CrossRef]

44. Bard Ermentrout. 1998. Linearization of F-I Curves by Adaptation. *Neural Computation* **10**:7, 1721-1729. [Abstract] [PDF] [PDF Plus]

45. Bard Ermentrout. 1998. *Reports on Progress in Physics* **61**, 353-430. [CrossRef]

46. Bo Cartling. 1996. Response Characteristics of a Low-Dimensional Model Neuron. *Neural Computation* **8**:8, 1643-1652. [Abstract] [PDF] [PDF Plus]

47. Isaac Meilijson, Eytan Ruppin. 1996. Optimal firing in sparsely-connected low-activity attractor networks. *Biological Cybernetics* **74**, 479-485. [CrossRef]